

PEV Fast-Charging Station Siting and Sizing on Coupled Transportation and Power Networks

Hongcai Zhang, *Student Member, IEEE*, Scott J. Moura, *Member, IEEE*, Zechun Hu, *Member, IEEE*, and Yonghua Song, *Fellow, IEEE*

Abstract—Plug-in electric vehicle (PEV) charging stations couple future transportation systems and power systems. That is, PEV driving and charging behavior will influence the two networks simultaneously. This paper studies optimal planning of PEV fast-charging stations considering the interactions between the transportation and electrical networks. The geographical targeted planning area is a highway transportation network powered by a high voltage distribution network. First, we propose the capacitated-flow refueling location model (CFRLM) to explicitly capture PEV charging demands on the transportation network under driving range constraints. Then, a mixed-integer linear programming model is formulated for PEV fast-charging station planning considering both transportation and electrical constraints based on CFRLM, which can be solved by deterministic branch-and-bound methods. Numerical experiments are conducted to illustrate the proposed planning method. The influences of PEV population, power system security operation constraints, and PEV range are analyzed.

Index Terms—Plug-in electric vehicle, charging station, planning, capacitated flow-refueling location model, mixed integer programming.

I. INTRODUCTION

PLUG-IN electric vehicles with lower emissions and energy consumption than internal combustion engine vehicles are regarded as a promising tool to combat energy sustainability and climate change. Therefore, governments, automobile companies, energy corporations, etc., have made great efforts to promote PEV development [1].

A major barrier for PEV adoption is their limited driving range compared with internal combustion engine vehicles – known as “range anxiety” [2]. Therefore, it is vitally important to properly site PEV charging systems to ameliorate range anxiety. Generally, PEV charging can be divided into two categories: 1) Destination charging, which happens when a PEV arrives at its destination, including home charging, workplace

charging; 2) Urgent charging, which happens when a PEV is enroute and its state-of-charge (SoC) falls below a certain threshold. Because most of the customers’ daily mileages are below the PEVs’ drive range on the market, destination charging is the major energy supply method for PEVs. However, complementary PEV urgent charging is still necessary in case of long-distance driving demands, especially on highway networks [2]. Destination charging needs are mostly satisfied by distributed charging spots with low-power (or normal-power) chargers deployed in private or public parking lots, while urgent charging needs are mostly satisfied by fast-charging stations [3]. In recent years, both distributed charging and fast-charging stations have gained heavy investments. These investments are still insufficient to meet the growing PEV fleet. For example, in China another 4.8 million distributed charging spots and 12 thousand fast-charging stations are planned for construction by 2020 [4].

Since fast-charging stations couple transportation and power networks, their locations and sizes not only affect PEV driving behavior, but also significantly impact transportation and power network operation. Therefore, the planning of fast-charging stations should take both transportation and electrical constraints into consideration. The locations and sizes of fast-charging stations in a transportation network should satisfy PEV driving demands, while simultaneously ensuring the security operation constraints of power systems, e.g., distribution line current limits and nodal voltage limits. In addition, an appropriate fast-charging station planning method should minimize the investment costs of both charging stations and corresponding power grid upgrades.

PEV charging station planning has become a research hotspot over recent years. We can generally divide this literature into three categorical perspectives.

A. Transportation Approach

Planning of gasoline stations has been studied for decades and the corresponding methodologies have been adopted and redeveloped for PEV charging station planning. These methods can be further divided into three major methodologies: a) nodal demand-based planning [5]–[7]; b) transportation simulation-based planning [8], [9]; c) traffic flow-based planning [10]–[16]. The nodal demand-based planning methods assume PEV charging occurs on some geographical nodes of the target planning area and locate the charging stations to satisfy charging demand [5]–[7]. However, these

Manuscript received May 31, 2016; revised August 7, 2016; accepted September 27, 2016. Date of publication October 3, 2016; date of current version June 19, 2018. This work was supported in part by the National Natural Science Foundation of China under Grant 51477082, and in part by the National Basic Research Program of China under Grant 2013CB228202. Paper no. TSG-00731-2016.

H. Zhang, Z. Hu, and Y. Song are with the Department of Electrical Engineering, Tsinghua University, Beijing 100084, China (e-mail: zechunhu@tsinghua.edu.cn).

S. J. Moura is with the Department of Civil and Environmental Engineering, University of California at Berkeley, Berkeley, CA 94720 USA.

Color versions of one or more of the figures in this paper are available online at <http://ieeexplore.ieee.org>.

Digital Object Identifier 10.1109/TSG.2016.2614939

methods only consider the geographical straight line distances between charging nodes while the transportation network congestion constraints are ignored. The transportation simulation-based planning methods use simulation to estimate PEV charging demands. The simulations are often based on real world comprehensive individual travel survey data [8], [9]. Obtaining such data can be costly for some target planning areas. Considering the mobility behavior of PEVs, some researchers proposed traffic flow based planning methods [10]–[16]. These methods use origin-destination (OD) traffic flow to estimate charging demands. In [10], the flow capturing location model (FCLM) was proposed, which seeks to locate a certain number of stations on a transportation network in order to capture as much traffic flow (demands) as possible. FCLM does not consider the driving range constraint of PEVs. Reference [11] modified FCLM into the flow-refueling location model (FRLM) which uses a flow-refueling concept to consider driving range. FRLM and its modified versions were also utilized in [12]–[16]. Articles from the transportation perspective [5]–[16] ignore power system constraints and the planning results may need readjustment according to the practical power system conditions.

B. Electrical Approach

As a new type of power demand, the PEV charging station planning in power systems has also drawn much attention. Existing work usually aims to site charging stations in power systems to satisfy power system economic or security operation constraints, while minimizing the investment costs for the charging stations and corresponding power grid upgrades. In [17], a two-step screening method was developed to locate charging stations in a distribution network and a modified primal-dual interior point algorithm was proposed to determine sizing. Reference [18] presents a framework for optimal design of battery charging/swapping stations in distribution networks based on life cycle cost analysis. In [19], the optimal sizing and siting of a PEV charging station with vehicle-to-grid capabilities in distribution networks was studied. In [20], a multi-objective optimization problem was developed to obtain the optimal siting and sizing of charging stations and renewable energy sources in distribution networks. References [17]–[20] ignored the transportation constraints and the results may need readjustment according to the practical transportation conditions.

C. Multidisciplinary Approach

There are few published papers that have studied PEV charging station planning considering both transportation and electrical constraints. In [21], an equilibrium modeling framework was proposed in a coupled transportation and power network. He *et al.* [21] assumed the transmission nodal electricity prices will influence PEV charging choices and therefore influence the traffic flow. However, the nodal electricity prices may hardly influence traffic flow since there is usually a long geographical distance between two transmission nodes and the costs for a PEV to travel from one

node to another is high. In [22], a multi-objective PEV charging station planning method was proposed to ensure charging service while reducing power losses and voltage deviations in distribution networks. The FCLM was used and a heuristic simulation procedure was adopted to consider driving range constraints. Yao *et al.* [23] studied coordinated planning for integrated power distribution networks and PEV charging systems based on a multi-objective evolutionary algorithm. The authors used the FCLM to consider transportation constraints, while the driving range constraint was ignored. Additionally, [22] and [23] consider low voltage distribution networks with service radiuses much smaller than a typical PEVs' driving range, so that the optimality of the planning results was not guaranteed. Reference [24] proposed a mixed-integer non-linear programming model for optimal siting and sizing of PEV charging stations solved by a genetic algorithm. The PEV charging demands were simply assumed to be uniformly distributed across the target area. Luo *et al.* [25] studied charging station siting which balances the benefits of PEV owner, charging station owner, and power grid operator. The effect of PEV charging on the power grid was simply assumed to be proportional to the charging power.

This paper studies optimal planning of highway PEV fast-charging stations utilizing a multidisciplinary approach, where both transportation and electrical constraints are considered. The planning objective is to increase social welfare and we assume the social planner has access to both transportation and power system information. The geographical targeted planning area is a highway transportation network powered by a high voltage distribution network with large service radius. Compared with the published literature, the major innovations of this paper are twofold:

- 1) A capacitated flow-refueling location model (CFRLM) is proposed, in which the PEVs' driving range constraint is explicitly incorporated. CFRLM utilizes OD traffic flows to estimate PEV charging demands and adopts queuing theory to model service abilities of PEV charging stations on the transportation network.
- 2) A mixed-integer linear programming (MILP) model for fast-charging station planning in coupled transportation and distribution networks is formulated, which can be solved by deterministic branch-and-bound methods. The planning model can optimize investment costs for both charging stations and distribution networks. The transportation constraints of CFRLM and the security operation constraints of the distribution network are considered simultaneously.

Numerical experiments are also conducted to validate the proposed planning method. The influences of various factors, such as PEV population, power system security operation constraints, PEV driving range, and PEV arrival/departure *SoCs* are also analyzed.

The CFRLM is formulated in Section II. Section III introduces the mixed-integer linear programming model for highway fast-charging station planning. Case studies are described in Section IV. Section V provides conclusions and discussions.

TABLE I
NOTATIONS USED IN THE CFRLM

i, j	Index of nodes for original transportation network. $i, j \in \Psi_q^{\text{tn}}$
(i, j)	Index of arcs from node i to node j . $(i, j) \in A_{(q)}$
q	Index of paths of the transportation network. $q \in Q$
Ψ_q^{tn}	Set of nodes of the original network (on path q).
$\hat{\Psi}_q^{\text{tn}}$	Set of nodes of the expanded network (on path q).
$A_{(q)}$	Set of arcs of the original network (on path q).
$\hat{A}_{(q)}$	Set of arcs of the expanded network (on path q).
$d_{i,j}$	Distance between node i and node j .
$F_{(q)}$	Volume of traffic flow (on path q).
$Q_{(i)}$	Set of paths of the original network (travel through node i).
R	Driving range of PEVs, in km.
SoC_a	Arrival SoC of a PEV at the origin node of a path.
SoC_d	Departure SoC of a PEV at the destination node of a path.
$c_{1,i}$	Fixed costs for building a new charging station at node i , including buildings costs etc.
$c_{2,i}$	Costs for adding an extra charging spot in a station at node i , including land use costs, charging spot purchase costs etc.
c_p	Penalty for unsatisfied charging demand.
$g(y_i)$	Charging service ability, given y_i charging spots.
\hat{y}_i	Maximum possible number of charging spots in station i .
s_i	Binary variable denoting charging station location at node i : $s_i = 1$, if there is a station at node i ; $s_i = 0$, otherwise.
x_{ij}^q	Continuous variable, fraction of OD flow on arc (i, j) , path q .
y_i	Integer variable, number of charging spots in station at node i .



II. CAPACITATED FLOW-REFUELING LOCATION MODEL

The proposed CFRLM is based on the flexible formulation of FRLM proposed in [12] and used in [16]. Compared with [12] and [16], the advantages of CFRLM are twofold. First, the service capacities of charging stations are considered in CFRLM. Since a PEV charging station's investment costs and maximum charging power are relevant to its capacity, i.e., number of charging spots, considering capacitated charging stations makes the planning model more practical. To define the service ability of each charging station, queuing theory is implemented in CFRLM. Secondly, we enable unsatisfied charging demand. Specifically, satisfying charging demand may be infeasible due to limited distribution line capacity. There, we utilize a penalty term to penalize the unsatisfied charging demands in CFRLM.

A. Driving Range Logic & Transportation Network Expansion

In this part, we review the driving range constraint logic (or refueling logic) and the corresponding transportation network expansion technique in [12], which are the foundations of CFRLM. The corresponding notations can be found in Table I.

We take a simple transportation network $G(\Psi_q^{\text{tn}}, A_q)$ in Fig. 1(a) as an example, which has a single travel path, i.e., path q . The path has 4 transportation nodes, i.e., $\Psi_q^{\text{tn}} = \{A, B, C, D\}$, and 3 arcs, i.e., $A_{(q)} = \{(A, B), (B, C), (C, D)\}$. A flow of PEVs, i.e., F_q , with driving range $R = 100$ km after a single charge need to travel from origin node A to destination node D without running out of energy. The PEVs enter the transportation network at node A with $SoCs$ equal to SoC_a and they need to leave the transportation network at node D

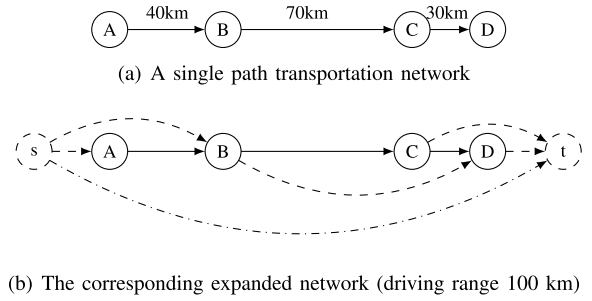


Fig. 1. An example of the transportation network expansion.

with $SoCs$ higher than SoC_d .¹ The planner's objective is to locate charging stations in the candidate location set Ψ_q^{tn} to satisfy the driving demands.

The original transportation network, i.e., $G(\Psi_q^{\text{tn}}, A_q)$ (see Fig. 1(a)), is expanded into a new network, i.e., $G(\hat{\Psi}_q^{\text{tn}}, \hat{A}_q)$ (see Fig. 1(b)), by the following steps:

- 1) Add source node s before the origin node A and a sink node t after the destination node D . Define $\hat{\Psi}_q^{\text{tn}} = \Psi_q^{\text{tn}} \cup \{s, t\}$.
- 2) Add two pseudo arcs, i.e., $\{s, A\}$ and $\{D, t\}$. And let distance $d_{s,A} = (1 - SoC_a) \times R$ and $d_{D,t} = SoC_d \times R$.
- 3) Define the ordering index of each node in $\hat{\Psi}_q^{\text{tn}}$ on path q as its index number from the source node s . For example, A is the second node on path q : $s-A-B-C-D-t$ and its ordering index is 2. Connect any two nodes, say i and j , in $\hat{\Psi}_q^{\text{tn}}$ by a pseudo arc if the ordering index of node i is less than that of node j , and node j can be reached from node i after a single charge. For network $G(\Psi_q^{\text{tn}}, A_q)$, the pseudo arcs (s, B) , (B, D) , (C, t) are added.
- 4) Add a new pseudo arc (s, t) to the network and let $\hat{A}_q = A_q \cup \{(s, A), (s, B), (B, D), (C, t), (D, t), (s, t)\}$.

In the expanded network $G(\hat{\Psi}_q^{\text{tn}}, \hat{A}_q)$, each path from s to t (excluding path $\{s, t\}$) characterizes a feasible solution for the charging station locations in the node set Ψ_q^{tn} . For example, the PEV traffic flow can travel through path $\{s, B, D, t\}$ on the condition that charging stations are located at B and D . Note that PEV traffic flow along path q requires at least one station located in Ψ_q^{tn} . The planner's objective is to locate some stations in Ψ_q^{tn} so that the PEV traffic flow can find a path in the expanded network $G(\hat{\Psi}_q^{\text{tn}}, \hat{A}_q)$ to travel from s to t . If there is no feasible set due to budget limits or distribution network constraints, the traffic flow must travel through the pseudo path $\{s, t\}$, on which no charging station is needed. This path captures unsatisfied charging demands. In summary, this expanded transportation network model incorporates PEV driving range constraints.

For a network with multiple paths, i.e., $G(\Psi^{\text{tn}}, A)$, the same expansion method is used for each path, rendering a corresponding expanded network, i.e., $G(\hat{\Psi}^{\text{tn}}, \hat{A})$.

¹ SoC_d corresponds to the distance between the driver's destination and the exit of the transportation network.

B. Capacitated Flow Refueling Location Model

Based on the expanded network, the CFRLM can be formulated as follows (see Table I for the corresponding notations):

$$\begin{aligned}
 & \min_{\{s_i, y_i, x_{ij}^q\}} \left\{ \sum_{i \in \Psi^{\text{tn}}} (c_{1,i} s_i + c_{2,i} y_i) + \sum_{q \in Q} c_p x_{st}^q F_q \right\} \quad (1) \\
 & \text{subject to:} \quad \sum_{j | (i,j) \in \hat{A}^q} x_{ij}^q - \sum_{j | (j,i) \in \hat{A}^q} x_{ji}^q = \begin{cases} 1, & i = s \\ -1, & i = t \\ 0, & i \neq s, t \end{cases}, \quad \forall q \in Q, \forall i \in \hat{\Psi}_q^{\text{tn}}, \quad (2) \\
 & x_{ij}^q \geq 0, \quad \forall q \in Q, \forall (i,j) \in \hat{A}_q, \quad (3) \\
 & \sum_{q \in Q} \sum_{j | (j,i) \in \hat{A}^q} F_q x_{ji}^q \leq g(y_i), \quad \forall i \in \Psi^{\text{tn}}, \quad (4) \\
 & y_i \leq \hat{y}_i s_i, \quad \forall i \in \Psi^{\text{tn}}, \quad (5) \\
 & y_i \in \mathbb{Z}, \quad \forall i \in \Psi^{\text{tn}}, \quad s_i \in \{0, 1\}, \quad \forall i \in \Psi^{\text{tn}}. \quad (6)
 \end{aligned}$$

The first term in objective function (1) is the summation of investment costs for each charging station, including a fixed cost per station and cost per number of charging spots. The second term in (1) is the monetary penalty for unsatisfied charging demands, which is proportional to the traffic flow traveling directly through the pseudo source and sink arcs, i.e., $x_{st}^q F_q$.

Equations (2)–(3) define the traffic flow equilibrium constraints, which ensure that the outflow minus inflow must equal the virtual supply and demand of the node. Equation (4) is the service ability constraint for each charging station. The traffic flow path can include a given node only if there is a charging station and enough charging spots are installed. Equation (5) upper-bounds the number of charging spots, if there is a charging station at that node.

Given the distribution of charging demands and charging service time, the service ability of a charging station is a function of the number of charging spots, i.e., $F = g(y)$ in constraint (4). For simplicity, a planner may assume linear relationship $g(y) = Ay$, in which A is the amount of charging demands each charging spot can satisfy. This assumption was used in previous work, such as [26]. To enhance the model accuracy, we use queuing theory [27] to estimate $g(y)$ in this paper.² And since $g(y)$ is nonlinear and convex, it makes the constraint (4) concave and thus the CFRLM is non-convex and difficult to scale. Thus, we use piecewise linearization [28] to reformulate constraint (4) into a mixed integer linear constraint. Details of the queuing modeling and piecewise linearization is given in the Appendix.

In practice, the charging stations can be located at any place in the transportation network, producing an infinite dimensional planning problem. This is intractable. In CFRLM, the

charging stations can only be located at predefined transportation nodes, i.e., Ψ_n^{tn} . To increase modeling accuracy, we can add auxiliary nodes on the long original arcs in the network - thus increasing the network granularity. As a result, the expanded transportation network has more nodes and the arc distances are decreased. Charging stations can be located at the original and auxiliary nodes, along the original arcs.

III. CHARGING STATION PLANNING MODEL

This section expands the CFRLM into a mixed integer linear programming planning model considering coupled transportation and power network constraints. When the PEV traffic flow is small, the PEV fast-charging load is small and has negligible impact on the power system. However, with rapidly increasing PEV adoption, the fast-charging power will grow significantly and may threaten secure operation of power distribution networks. This will be particularly predominant in a highway transportation network, where the covered area is mostly rural and loads are traditionally low. PEV fast-charging loads may become a major part of the total power demand.

We study PEV charging station planning in 110 kV high voltage distribution networks, to directly address limited PEV driving range. In practice, PEV charging stations are usually connected to medium voltage distribution networks, e.g., 10 kV networks in China. The planning results can be further adjusted for the lower voltage distribution networks, for which the previous works in [22] and [23] can be used.

A. Planning Objective

The planning model objective is to minimize investment costs, subject to satisfying PEV charging demand, formulated as follows (see Table II for the corresponding notations):

$$\min_{\{s_i, y_i\}} \{C_{\text{sta}} + C_{\text{gri}} + C_{\text{pen}}\} \quad (7)$$

where:

$$C_{\text{sta}} = \sum_{i \in \Psi^{\text{tn}}} (c_{1,i} s_i + c_{2,i} y_i) \quad (8)$$

$$C_{\text{gri}} = \sum_{i \in \Psi^{\text{tn}}} (c_{3,i} l_i P_i + c_{4,i} P_i^{\text{sub}}) \quad (9)$$

$$C_{\text{pen}} = \sum_{q \in Q} c_p x_{st}^q F_q \quad (10)$$

where, the first term and the third term in (7) respectively represent the charging station investment costs, i.e., C_{sta} , and the penalty for unsatisfied charging demands, i.e., C_{pen} , in CFRLM. The second term in (7) accounts for power distribution network costs, i.e., C_{gri} . This includes the costs for distribution lines, i.e., the first term in (9), and the costs for substation capacity expansion, i.e., the second term in (9). Note that the three terms in (7) have the same unit.

The distribution line investment cost is approximately proportional to the product of maximum charging station power, i.e., P_i , and the required distribution line length, i.e., l_i [29]. P_i can be calculated as:

$$P_i = p y_i, \quad \forall i \in \Psi^{\text{tn}}. \quad (11)$$

²We can also adopt more accurate simulations or empirical data to estimate $g(y)$ in practice.

TABLE II
NOTATIONS USED IN THE PLANNING MODEL

b	Index of branches of the distribution network. $b \in \Psi^{\text{db}}$
n	Index of nodes of the distribution network. $n \in \Psi^{\text{dn}}$
Ψ^{db}	Set of branches of the distribution network.
Ψ^{dn}	Set of nodes of the distribution network.
Ψ_n^{tn}	Set of transportation nodes connected to distribution node n .
B	Investment costs budget.
$c_{3,i}$	Per-unit costs for distribution line at location i , in \$(/(\text{kVA}\cdot\text{km})\$.
$c_{4,i}$	Per-unit costs for substation capacity expansion at i , in \$/kVA.
d_n^{base}	Base load current at distribution node n .
\mathbf{d}^{base}	Column vector of nodal base load current, $[d_n^{\text{base}}]^T$.
\bar{f}_b	Upper limit of branch current of branch b .
g_n	Generation current injection at distribution node n .
\mathbf{g}	Column vector of the nodal generation injection, $[g_n]^T$.
l_i	Required distribution line length to install a charging station at location i .
p	Rated charging power of a charging spot.
$P_{i,0}^{\text{sub}}$	Initial substation capacity available at transportation node i .
\mathbf{S}	Node-branch incidence matrix for the distribution network.
$\underline{V}_n/\bar{V}_n$	Lower/upper limit of nodal voltage at distribution node n .
z_b	Impedance of branch b .
d_n^{ev}	PEV charging current at distribution node n .
\mathbf{d}^{ev}	Column vector of nodal PEV charging current, $[d_n^{\text{ev}}]^T$.
f_b	Current of branch b .
\mathbf{f}	Column vector of branch current, $[f_b]^T$.
P_i	Maximum PEV charging power at transportation node i .
P_i^{sub}	Substation capacity expansion at transportation node i .
V_n	Nodal voltage at distribution node n .
\mathbf{V}	Column vector of the nodal voltage, $[V_n]^T$.
\hat{V}	Reference voltage of the distribution network.

In practice, the required distribution line length must be determined for each candidate location.

In some locations, existing power substations have sufficient capacity to supply added PEV charging stations. If the existing substation capacity is insufficient, then the substation must be expanded. Let $P_{i,0}^{\text{sub}}$ denotes the surplus substation capacity at location i . Then the required substation capacity expansion can be calculated as:

$$P_i^{\text{sub}} = \max(0, P_i - P_{i,0}^{\text{sub}}), \quad \forall i \in \Psi^{\text{tn}}. \quad (12)$$

B. Planning Constraints

1) *Transportation Constraints*: The planning model must satisfy CFRLM constraints (2)–(6).

2) *Kirchhoff's Law Constraints* [30]: The branch currents and nodal voltages of the distribution network must satisfy Kirchhoff's Current Law (KCL) and Kirchhoff's Voltage Law (KVL), which are defined respectively as follows:

$$\mathbf{S}\mathbf{f} + \mathbf{g} = \mathbf{d}^{\text{ev}} + \mathbf{d}^{\text{base}}, \quad (13)$$

$$z_b f_b + [\mathbf{S}]_{\text{row } b}^T \mathbf{V} = 0, \quad \forall b \in \Psi^{\text{db}} \quad (14)$$

in which, the PEV charging current at distribution node n is the summation of all the charging current at its coupled transportation nodes:

$$d_n^{\text{ev}} = \sum_{i \in \Psi_n^{\text{tn}}} P_i / \hat{V}, \quad \forall n \in \Psi^{\text{dn}}. \quad (15)$$

The KCL and KVL constraints provide a linear approximation of the optimal power flow constraints in distribution networks, which was also used in [30].

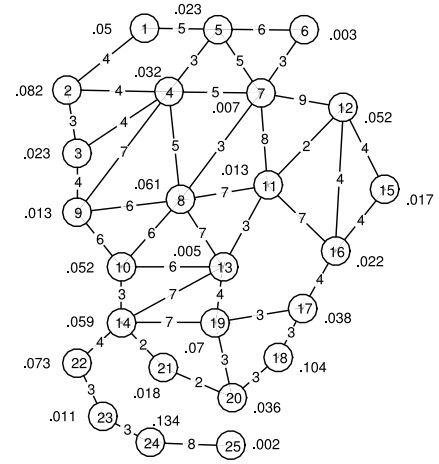


Fig. 2. A 25-node transportation network used for the case study.

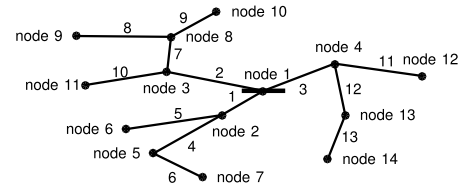


Fig. 3. A 110 kV distribution network used for the case study.

3) *Distribution Line Current and Nodal Voltage Limits*: The distribution line currents and nodal voltages must not violate their permitted ranges, which are respectively defined as follows:

$$|f_b| \leq \bar{f}_b, \quad \forall b \in \Psi^{\text{db}}, \quad (16)$$

$$\underline{V}_n \leq V_n \leq \bar{V}_n, \quad \forall n \in \Psi^{\text{dn}}. \quad (17)$$

4) *Budget Constraint*: In some scenarios, the total affordable investment costs of the PEV charging system planner is limited, and defined as follows:

$$C_{\text{sta}} + C_{\text{gri}} \leq B. \quad (18)$$

IV. CASE STUDIES

A. Case Overview and Parameter Settings

We consider a 25-node highway transportation network [31] coupled with a 14-node 110 kV high voltage distribution network to illustrate the proposed planning method.

The 25-node transportation system is depicted in Fig. 2. The number on each arc represents the distance between the corresponding two nodes. We assume the per-unit distance in Fig. 2 is 10 km. For example, the distance of arc (1, 2) is 4 units, corresponding to 40 km. The decimal next to each node is the node's weight, i.e., W , which represents its traffic flow gravitation [31]. The gravity spatial interaction model was used to generate an OD flow structure based on node weights and arc distances [10]:

$$F_{ij} = (1.5W_iW_j)/d_{ij}, \quad \forall i, j, i \neq j \quad (19)$$

$$F_{ij}^{\text{PEV}} = F_{\text{total}}^{\text{PEV}} \times F_{ij} / \sum_{i \neq j} F_{ij}, \quad \forall i, j, i \neq j \quad (20)$$

where $F_{\text{total}}^{\text{PEV}}$ is the total PEV traffic flow (average number of PEVs that travel through this transportation network) during

TABLE III
NODE COUPLING RELATIONSHIP OF THE TWO NETWORKS

Distribution Node ID	01	02	03	04	05	06	07
Transportation Node ID	—	13	08	12	22	14	24
Distribution Node ID	08	09	10	11	12	13	14
Transportation Node ID	04	02	05	09	15	17	20

peak hour, in h^{-1} ; F_{ij}^{PEV} is the PEV traffic flow from node i to node j , in h^{-1} .

To enhance network granularity, we add extra auxiliary nodes on the arcs with distances longer than 20 km. As a result, the modified transportation network has 93 nodes and the longest distance of all arcs is 20 km. The charging stations can be located at the original and auxiliary nodes. The weights of auxiliary nodes were set to 0.

The diagram of the 110 kV high voltage distribution network is shown in Fig. 3. We assume node 1 is connected to a 220 kV/110 kV transformer with 150 MVA capacity. Due to limited space, the parameters of the distribution network are omitted in this paper, but can be downloaded in https://github.com/zhanghc09/PEV-charging-network-planning/blob/master/110kV_distribution_system.pdf. The node coupling relationship between the distribution and transportation network is recorded in Table III. We assume the transportation nodes not included in Table III are connected to the nearest distribution nodes geographically. The voltage constraints are $V_n = 0.95$ and $\bar{V}_n = 1.05$, and the branch current limits are set at their rated capacities.

The PEV driving range after a charge, i.e., R , is assumed to be 200 km and the energy consumption is 0.14 kWh/km.³ The rated charging power for each charging spot (p) is 44 kW, and the charging efficiency (η) is 92% [7]. Consequently, the average service time to recharge a PEV with empty battery is about $\mu = (200 \text{ km} \times 0.14 \text{ kWh/km}) / (92\% \times 44 \text{ kW}) = 42$ minutes. The service time's coefficient of variance, i.e., c_s^2 , is assumed to be 0.5 to reflect the influence of stochastic driving/charging behaviors, energy consumptions etc. In practice, the PEV charging power is not constant and a typical charging process usually includes two stages: 1) the constant current charge, when the battery is charged around its rated charging power; 2) the constant voltage charge, when the charging power decreases gradually to top off batteries [32], [33]. Because the constant voltage stage is quite time-consuming, Tesla recommends its customers to charge PEVs only at the first stage, i.e., charge PEVs to about 80% SoCs, to save time [33]. Reference [32] also shows that charging PEVs at the constant voltage stage would under-utilize the station's service ability during peak charging demand intervals. Therefore, we assume that all the customers only charge their PEVs at the first stage in highway networks to save time, so that the charging power can be regarded to be constant.

We assume the maximum permitted average waiting time $\bar{T} = 10$ minutes. The arrival SoC and departure SoC for all paths in the transportation network are assumed to be both

³ R is not necessarily equal to the drive range after getting fully recharged. In highway networks, PEVs are not likely to get fully recharged at charging stations, which is explained later in this paragraph.

50%, thereby forcing at least one charging event. The maximum number of spots in each charging station, i.e., \hat{y}_i , is assumed to be 200. In practice, \hat{y}_i can be defined according to land use limitation etc.

The fixed costs for each PEV charging station is assumed to be $c_{1,i} = \$163,000$. The land use costs is 407 $\$/\text{m}^2$ and adding one extra charging spot requires 20 m^2 land. Per-unit purchase cost for one charging spot is $\$23,500$ [7]. Thus we have $c_{2,i} = 407 \text{ } \$/\text{m}^2 \times 20 \text{ m}^2 + \$23,500$. The distribution line cost is assumed to be $c_{3,i} = 120 \text{ } \$/(\text{kVA} \cdot \text{km})$ [34]. The distance from the PEV charging station to its nearest low/medium voltage substation, i.e., l_i , is assumed to be 10% of the distance between the PEV charging station and its nearest 110 kV distribution node. The substation expansion cost is assumed to be $c_{4,i} = 788 \text{ } \$/\text{kVA}$ [23]. In practice, the land use and labor costs vary by location. To model this feature across nodes, the per-unit costs, i.e., $c_{1,i}$, $c_{2,i}$ and $c_{4,i}$, at each location i are assumed to be greater than the base values introduced above by $5W_i \times 100\%$. We assume each original transportation node has 1 MVA surplus substation capacity which can be utilized by charging stations, while the auxiliary nodes have no spare substation capacity. The per-unit penalty cost for unsatisfied charging demand $c_p = \$10^4$ and the budget constraint $B = \infty$. These parameter values are for illustration and not necessarily representative of a particular transportation/power system network.

Because there are 93 candidate charging station locations, the investment variables include 93 integer variables, i.e., y , and 93 binary variables, i.e., s . We used three linear segments to approximate the nonlinear function $g(y)$ in (4). As a result, a total of $93 \times 4 = 372$ binary variables and 372 continuous variables are introduced to reformulate (4) (see Appendix). The other variables are all continuous including the traffic flow, i.e., x , voltages, i.e., V , etc. with a total number of 33,340. The constraint number is 7,853. Note that the scale of the problem is mainly determined by the scales of the transportation and distribution networks (integer and binary variables). PEV driving range and arrival/departure SoCs may influence the structure of the expanded network and therefore influence the scale of the continuous traffic flow variables, i.e., x . For example, longer drive range leads to more complex expanded transportation network, and as a result, a larger scale problem. However, because PEV driving range and arrival/departure SoCs are only related to continuous variables, their influences are not significant. The scale of PEV traffic flow cannot influence the scale of the problem. We used CPLEX [35] to solve the optimal PEV charging station planning problem on a laptop with a quad-core Intel Core i7 processor and 8 GB memory. It takes about 40 minutes to solve one single planning problem described above with a 0.5% convergent gap.

B. Planning Results and Analysis

PEV charging station planning results under different peak hour PEV traffic flows are demonstrated in Fig. 4. The planning results for the 1,000 and 1,500 PEVs/h scenarios are summarized in Table IV, the locations of the stations in the transportation network are demonstrated in Fig. 5 and Fig. 6,

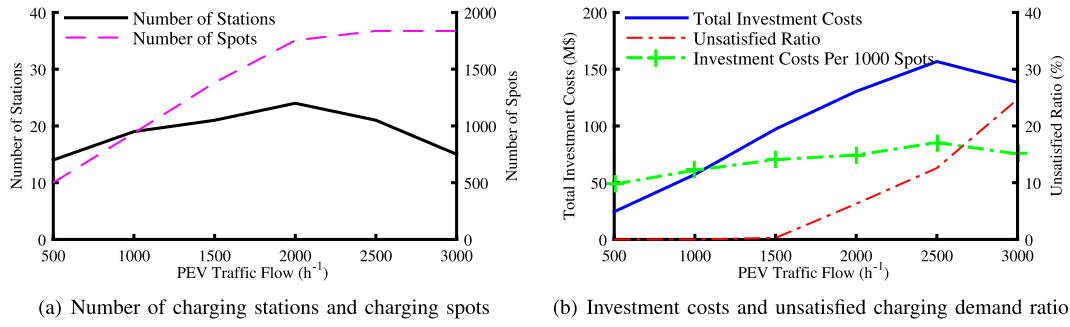


Fig. 4. Planning results under different PEV traffic flow scenarios.

TABLE IV
PLANNING RESULTS SUMMARY (1000 AND 1500 PEVS/H)

PEVs (h ⁻¹)	No. of Stations	No. of Spots	Investment costs (M\$)			Unsatisfied Demand
			Station	Grid	Total	
1000	19	938	35.03	22.22	57.25	0.00 %
1500	21	1382	50.37	46.83	97.20	0.28 %

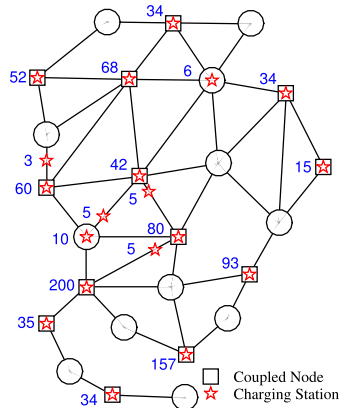


Fig. 5. Station locations (1000 PEVs/h).

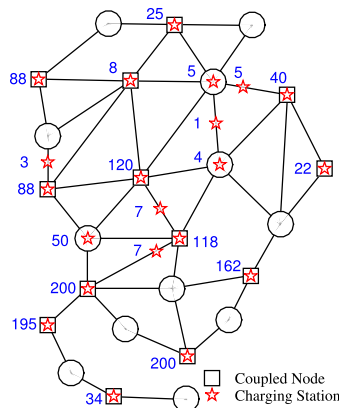
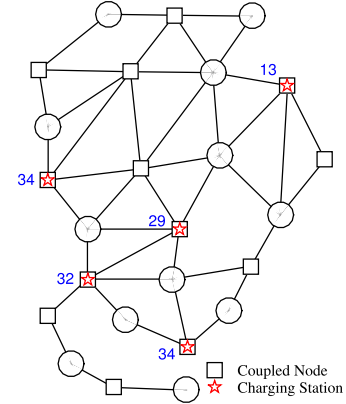


Fig. 6. Station locations (1500 PEVs/h).

in which the corresponding number of charging spots are labeled for each station. Note that the station locations in the distribution network can be obtained according to the coupling relationship in Table III.

As expected, the number of spots grows with PEV traffic flow. When the PEV traffic flow grows beyond 1,500 PEVs/h,

Fig. 7. Station locations ($R=400$ km).TABLE V
CONGESTION LEVEL OF DISTRIBUTION LINES (1500 PEVS/H)

Line ID	01	02	03	04	05	06	07
Level (%)	94.4	99.9	63.8	58.6	76.1	22.7	89.6
Line ID	08	09	10	11	12	13	
Level (%)	62.3	11.4	29.0	14.5	75.6	57.8	

the charging demands can no longer be fully satisfied due to the distribution network's operation constraints. The maximum number of charging spots in the system is about 1,800. In this case, the active constraints are the distribution line current limits, i.e., (16). The congestion level, i.e., the ratio of the actual line current to the corresponding line capacity, of each distribution line in the 1,500 PEVs/h scenario is listed in Table V. Line 02's current reaches to its upper limit.

Unlike spots, the number of charging stations begin to decrease with the growth of PEV traffic flow when the latter is beyond 2,000 PEVs/h. When the PEV traffic flow is low, the planning model locates charging stations to satisfy all the charging demands because the penalty for unsatisfied charging demands is high. Therefore, the number of charging stations tends to increase with traffic flow. However, when the traffic flow increases beyond the system's capacity, the planning model only locates fewer centralized charging stations (on the premise that the charging stations and the distribution system are still fully utilized in order to 1) decrease the fixed costs in objective (8) and 2) build charging stations at low costs nodes. This phenomenon can also be visualized by

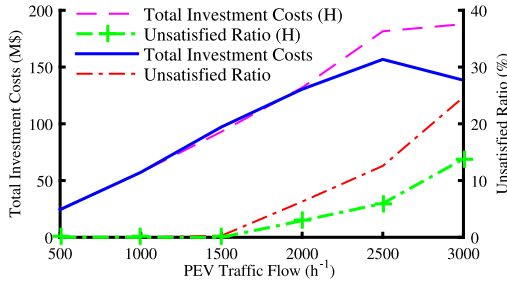


Fig. 8. Planning results under nominal case in Fig. 4(b) and high capacity distribution lines (H, increased by 10%).

the average investment costs for every 1,000 charging spots in Fig. 4(b). At the first stage (500–2,000 PEVs/h), the average investment costs per spot increase with the growth of PEV traffic flow because the planning constraints force new charging stations to be built in higher costs areas. And then the average investment costs per spot decrease at the second stage (2,500–3,000 PEVs/h) since the number of charging stations reduces. As a result, the total investment costs decreases after the traffic flow grows higher than 2,500 PEVs/h (note that the unsatisfied charging demand ratio also rises which leads to significant penalty costs).

C. Sensitivity Analysis

1) *Distribution Network Constraints*: As discussed in Section IV-B, the distribution network constraints limit the service ability of the total charging system in the transportation network. Since distribution lines are the most expensive elements in a distribution network, we increased each distribution line's capacity by 10% and compared the results in Fig. 8. When the capacities are increased, more charging demand can be satisfied as traffic flow increases beyond 1,500 PEVs/h. This sensitive analysis can provide guidance for power grid upgrades.

2) *Driving Range After A Charge*: As battery technology and manufacturing mature, PEV driving range will increase with battery capacity. Planning results under different PEV driving range scenarios are demonstrated in Fig. 9. We assume the PEVs have driven for 100 km before arriving at the transportation network and they need to drive another 100 km after they depart from the network before arriving their destinations. As expected, the investment costs and unsatisfied demand decrease with increasing range. When the PEVs' driving range after a charge is higher than 500 km, constructing charging stations are not necessary in this system. The station locations and their corresponding configurations are demonstrated in Fig. 7 under the scenario of 400 km driving range.

3) *State-of-Charge*: The arrival SoCs depend on the distances PEVs travel before arriving to the transportation network. The departure SoC depends on the distances PEVs travel to their destinations after leaving the transportation network. Required PEV investment costs under different SoC_a and SoC_d are visualized in Fig. 10. The higher the SoC_a is, the lower the investment costs are and conversely the lower the SoC_d is, the lower the investment costs are. In practice, SoC_a and SoC_d

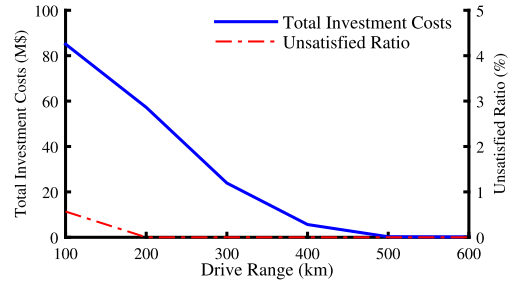


Fig. 9. Influence of driving range (1000 PEVs/h).

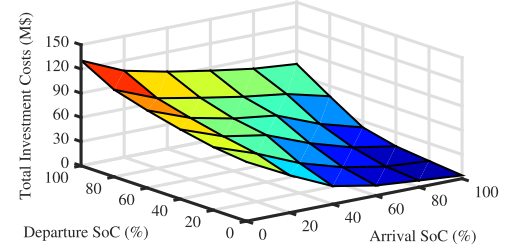


Fig. 10. Influence of arrival and departure SoC (1000 PEVs/h).

TABLE VI
INFLUENCE OF MAXIMUM ARC LENGTH

Maximum arc length (km)	10	20	30	40	50
Total costs (M\$)	55.20	57.25	57.48	58.40	58.61

should be obtained by investigating the PEV mobility before arriving and after leaving the transportation network. Without this information, the planner can use low SoC_a and high SoC_d to make a worst-case planning decision.

4) *Maximum Arc Length*: As we have introduced in CFRLM, we can divide long arcs into short arcs by adding auxiliary nodes (candidate locations). Decreasing maximum arc length increases the candidate charging station siting granularity (see Table VI). However, increasing candidate locations increases the optimization program size. The PEV charging network planner should appropriately select the maximum arc length to balance granularity with problem complexity.

V. CONCLUSION

This paper studies PEV fast-charging station siting by considering the coupled interactions between the transportation and power networks. CFRLM is proposed to explicitly incorporate PEV driving range and OD traffic flow to estimate PEV charging demand. In addition, $M/M/s$ queuing is adopted to model each charging station's service ability. A mixed integer linear programming (MILP) model for the planning of PEV fast-charging stations in coupled transportation and high voltage distribution networks is proposed, using the CFRLM. We incorporate distribution network security operation constraints. Numerical experiments illustrate the effectiveness of the proposed method. Various sensitivities, such as PEV population, line capacity, driving range, arrival and departure SoCs, and network granularity have notable influences on the optimal planning results.

In practice, the PEV driving range and arrival/departure *SoCs* are respectively heterogeneous and stochastic. In the future, stochastic formulation of the CFRLM will be an important research focus. One possible method to extend the CFRLM into a stochastic model is to respectively generate an expanded transportation network for each type of PEV (divided by drive range and arrival/departure *SoCs* etc.). And the traffic flow equilibrium constraint (2) should be satisfied for each type of PEV, i.e., satisfied for each expanded transportation network. In this way, the CFRLM can be modeled as a stochastic programming model in which multiple types of PEVs' charging demands are satisfied. In this paper, all the PEVs are assumed to have uniform driving range and arrival/departure *SoC*. Note that, the planning model, based on this assumption, provides a feasible and conservative solution when we consider the shortest driving range, lowest arrival *SoC* and highest departure *SoC*.⁴ The solution can still provide meaningful guidance for PEV charging facility investments and help promote PEV adoption in practice.

In addition, this paper only considers peak OD traffic flows. In practice, one may consider dynamic OD traffic flows [36] to model charging demands for all time intervals. This added temporal granularity can increase model accuracy – a topic of future work.

APPENDIX

QUEUING MODELING AND PIECEWISE LINEARIZATION OF CONSTRAINT (4)

According to [32], the arrival of PEVs can be modeled as a Poisson process, with a parameter equal to its OD flow F , and parameter μ that characterizes average service time with a general distribution. The charging spots are assumed to be identical and PEVs are served based on the first-come first-served rule. Then the service ability of charging stations with different spot numbers can be modeled with an $M/G/s/k$ queue [32], in which M represents the Poisson process, G represents the general service time distribution, s represents the number of spots in a station, and k is the waiting spaces in a station. Highway fast-charging stations usually have sufficient waiting spaces so that we can assume $k = \infty$ for simplicity in the planning model, as discussed in [37]. Therefore, we adopt the $M/G/s$ queue [27] in this paper. When the distributions of traffic flow and service time are given at a charging station, the minimum required charging spot number is given by the following optimization model:

$$y = g^{-1}(F) = \min_{\{z\}} z \quad (21)$$

subject to:

$$EW(M/G/s) = \frac{EW(M/M/s)(1 + c_s^2)R_D}{(2R_D - 1)c_s^2 + 1} \leq \bar{T}, \quad (22)$$

⁴Note that it is not economic to design a charging network to satisfy all the possible charging demands. For example, some short-distance PEVs, which are only designed for short-distance urban commuting, are not supposed to be the target customers of charging stations on highway networks. Therefore, in practice, there should be proper entry thresholds for drive range and arrival *SoC* and an acceptable service standard for departure *SoC* on highway networks. And these thresholds and standard will be the input for the planning.

$$EW(M/M/s) = \frac{(z\rho)^z \rho}{Fz!(1-\rho)^2} \left[\sum_{k=0}^{z-1} \frac{(z\rho)^k}{k!} + \frac{(z\rho)^z}{z!(1-\rho)} \right]^{-1}, \quad (23)$$

$$R_D = \frac{1}{2} \left[1 + F(\theta) \frac{(1-\rho)}{\rho} \left(1 - e^{-\frac{\theta\rho}{F(\theta)(1-\rho)}} \right) \right], \quad (24)$$

$$F(\theta) = \frac{\theta}{8(1+\theta)} \left(\sqrt{\frac{9+\theta}{1-\theta}} - 2 \right), \quad (25)$$

$$\theta = \frac{z-1}{z+1}, \quad \rho = \frac{F}{z\mu} \quad (26)$$

where, $EW(M/G/s)$ is the average waiting time of the $M/G/s$ queue, \bar{T} is its upper limit, z is the number of charging spots, and c_s^2 is the coefficient of variance of the service time. $EW(M/G/s)$ is limited by equation (22) to guarantee service quality. Because $EW(M/G/s)$ decreases monotonously with the increase of z , problem (22)–(26) can be solved heuristically by traversing z . Interested readers can refer to [27] for detailed information.

Based on model (22)–(26), we can traverse the charging demand parameter F to obtain the corresponding minimum number of charging spots y (optimal z), thus providing $y = g^{-1}(F)$ and $F = g(y)$. Afterwards, we can use piecewise linearization to reformulate constraint (4) into a mixed integer linear constraint [28].

Assume that $g(y)$ is approximated by three linear segments:

$$F = g(y) = \begin{cases} a_1 + b_1 y, & c_1 \leq y \leq c_2 \\ a_2 + b_2 y, & c_2 \leq y \leq c_3 \\ a_3 + b_3 y, & c_3 \leq y \leq c_4 \end{cases} \quad (27)$$

where, a_i and b_i ($i = 1, 2, 3$) are the coefficients of the linear functions, and c_i ($i = 1, 2, 3, 4$) are the breakpoints. Then, by introducing four nonnegative continuous variables y_i and four binary variables B_i ($i = 1, 2, 3, 4$), the (27) can be equivalently reformulated as the following equations (28)–(33):

$$F = g(y) = \sum_{i=1}^4 g(c_i) y_i, \quad (28)$$

$$y = \sum_{i=1}^4 c_i y_i, \quad (29)$$

$$\sum_{i=1}^4 y_i = 1, \quad (30)$$

$$y_i \leq B_i, \quad \forall i \in \{1, 2, 3, 4\}, \quad (31)$$

$$\sum_{i=1}^4 B_i \leq 2, \quad (32)$$

$$B_i + B_j \leq 1, \quad \forall i, j \in \{1, 2, 3, 4\} \text{ and } |i - j| \neq 1. \quad (33)$$

By approximating the nonlinear function $g(y)$ by equations (28)–(33), the concave constraint (4) is reformulated into a set of mixed integer linear constraints. Piecewise linearization is a mature technique. Interested readers can refer to [28] for detailed information.

REFERENCES

- [1] Z. Xu, W. Su, Z. Hu, Y. Song, and H. Zhang, "A hierarchical framework for coordinated charging of plug-in electric vehicles in China," *IEEE Trans. Smart Grid*, vol. 7, no. 1, pp. 428–438, Jan. 2016.
- [2] T. Franke and J. F. Krems, "What drives range preferences in electric vehicle users?" *Transp. Policy*, vol. 30, pp. 56–62, Nov. 2013.
- [3] H. Zhang, Z. Hu, Z. Xu, and Y. Song, "Optimal planning of PEV charging station with single output multiple cables charging spot," *IEEE Trans. Smart Grid*, to be published, accessed on Feb. 15, 2016. [Online]. Available: <http://ieeexplore.ieee.org/document/7390308/>
- [4] Chinadaily. *China to Build 12,000 Nev Chargers by 2020*. Accessed on Apr. 20, 2016. [Online]. Available: http://www.chinadaily.com.cn/business/motoring/2015-10/13/content_22170160.htm
- [5] H. Xu, S. Miao, C. Zhang, and D. Shi, "Optimal placement of charging infrastructures for large-scale integration of pure electric vehicles into grid," *Int. J. Elect. Power Energy Syst.*, vol. 53, no. 1, pp. 159–165, 2013.
- [6] J. Cavadas, G. H. de Almeida Correia, and J. Gouveia, "A MIP model for locating slow-charging stations for electric vehicles in urban areas accounting for driver tours," *Transp. Res. E Logist. Transp. Rev.*, vol. 75, pp. 188–201, Mar. 2015.
- [7] H. Zhang, Z. Hu, Z. Xu, and Y. Song, "An integrated planning framework for different types of pev charging facilities in urban area," *IEEE Trans. Smart Grid*, vol. 7, no. 5, pp. 2273–2284, Sep. 2016.
- [8] H. Cai, X. Jia, A. S. F. Chiu, X. Hu, and M. Xu, "Siting public electric vehicle charging stations in Beijing using big-data informed travel patterns of the taxi fleet," *Transp. Res. D Transp. Environ.*, vol. 33, pp. 39–46, Dec. 2014.
- [9] N. Shahraki, H. Cai, M. Turkay, and M. Xu, "Optimal locations of electric public charging stations using real world vehicle travel patterns," *Transp. Res. D Transp. Environ.*, vol. 41, pp. 165–176, Dec. 2015.
- [10] M. J. Hodgson, "A flow-capturing location-allocation model," *Geogr. Anal.*, vol. 22, no. 3, pp. 270–279, 1990.
- [11] M. Kuby and S. Lim, "The flow-refueling location problem for alternative-fuel vehicles," *Socio Econ. Plan. Sci.*, vol. 39, no. 2, pp. 125–145, 2005.
- [12] S. A. MirHassani and R. Ebrazi, "A flexible reformulation of the refueling station location problem," *Transp. Sci.*, vol. 47, no. 4, pp. 617–628, 2013.
- [13] H.-Y. Mak, Y. Rong, and Z.-J. M. Shen, "Infrastructure planning for electric vehicles with battery swapping," *Manag. Sci.*, vol. 59, no. 7, pp. 1557–1575, 2013.
- [14] P.-S. You and Y.-C. Hsieh, "A hybrid heuristic approach to the problem of the location of vehicle charging stations," *Comput. Ind. Eng.*, vol. 70, pp. 195–204, Apr. 2014.
- [15] R. Riemann, D. Z. W. Wang, and F. Busch, "Optimal location of wireless charging facilities for electric vehicles: Flow-capturing location model with stochastic user equilibrium," *Transp. Res. C Emerg. Technol.*, vol. 58, pp. 1–12, Sep. 2015.
- [16] S. H. Chung and C. Kwon, "Multi-period planning for electric car charging station locations: A case of Korean Expressways," *Eur. J. Oper. Res.*, vol. 242, no. 2, pp. 677–687, 2015.
- [17] Z. Liu, F. Wen, and G. Ledwich, "Optimal planning of electric-vehicle charging stations in distribution systems," *IEEE Trans. Power Del.*, vol. 28, no. 1, pp. 102–110, Jan. 2013.
- [18] Y. Zheng *et al.*, "Electric vehicle battery charging/swap stations in distribution systems: Comparison study and optimal planning," *IEEE Trans. Power Syst.*, vol. 29, no. 1, pp. 221–229, Jan. 2014.
- [19] K. Khalkhali, S. Abapour, S. M. Moghaddas-Tafreshi, and M. Abapour, "Application of data envelopment analysis theorem in plug-in hybrid electric vehicle charging station planning," *IET Gener. Transm. Distrib.*, vol. 9, no. 7, pp. 666–676, Apr. 2015.
- [20] M. H. Moradi, M. Abedini, S. M. R. Tousi, and S. M. Hosseinian, "Optimal siting and sizing of renewable energy sources and charging stations simultaneously based on differential evolution algorithm," *Int. J. Elect. Power Energy Syst.*, vol. 73, pp. 1015–1024, Dec. 2015.
- [21] F. He, D. Wu, Y. Yin, and Y. Guan, "Optimal deployment of public charging stations for plug-in hybrid electric vehicles," *Transp. Res. B Methodol.*, vol. 47, pp. 87–101, Jan. 2013.
- [22] G. Wang, Z. Xu, F. Wen, and K. P. Wong, "Traffic-constrained multi-objective planning of electric-vehicle charging stations," *IEEE Trans. Power Del.*, vol. 28, no. 4, pp. 2363–2372, Oct. 2013.
- [23] W. Yao *et al.*, "A multi-objective collaborative planning strategy for integrated power distribution and electric vehicle charging systems," *IEEE Trans. Power Syst.*, vol. 29, no. 4, pp. 1811–1821, Jul. 2014.
- [24] P. Sadeghi-Barzani, A. Rajabi-Ghahnavieh, and H. Kazemi-Karegar, "Optimal fast charging station placing and sizing," *Appl. Energy*, vol. 125, pp. 289–299, Jul. 2014.
- [25] C. Luo, Y.-F. Huang, and V. Gupta, "Placement of EV charging stations: Balancing benefits among multiple entities," *IEEE Trans. Smart Grid*, to be published, accessed on Feb. 20, 2016. [Online]. Available: <http://ieeexplore.ieee.org/document/7368203/>
- [26] C. Upchurch, M. Kuby, and S. Lim, "A model for location of capacitated alternative-fuel stations," *Geogr. Anal.*, vol. 41, no. 1, pp. 127–148, 2009.
- [27] T. Kimura, "Approximations for multi-server queues: System interpolations," *Queueing Syst.*, vol. 17, no. 3, pp. 347–382, 1994.
- [28] M.-H. Lin, J. G. Carlsson, D. Ge, J. Shi, and J.-F. Tsai, "A review of piecewise linearization methods," *Math. Problems Eng.*, vol. 2013, 2013, Art. no. 101376.
- [29] W. Qi, Y. Liang, and Z.-J. M. Shen, "Joint planning of energy storage and transmission for wind energy generation," *Oper. Res.*, vol. 63, no. 6, pp. 1280–1293, 2015.
- [30] S. Haffner, L. F. A. Pereira, L. A. Pereira, and L. S. Barreto, "Multistage model for distribution expansion planning with distributed generation—Part I: Problem formulation," *IEEE Trans. Power Del.*, vol. 23, no. 2, pp. 915–923, Apr. 2008.
- [31] D. Simchi-Levi and O. Berman, "A heuristic algorithm for the traveling salesman location problem on networks," *Oper. Res.*, vol. 36, no. 3, pp. 478–484, 1988.
- [32] P. Fan, B. Sainbayar, and S. Ren, "Operation analysis of fast charging stations with energy demand control of electric vehicles," *IEEE Trans. Smart Grid*, vol. 6, no. 4, pp. 1819–1826, Jul. 2015.
- [33] Tesla. *Supercharger*. Accessed on Jul. 26, 2016. [Online]. Available: <https://www.tesla.com/supercharger>
- [34] W. Yao, C. Y. Chung, F. Wen, M. Qin, and Y. Xue, "Scenario-based comprehensive expansion planning for distribution systems considering integration of plug-in electric vehicles," *IEEE Trans. Power Syst.*, vol. 31, no. 1, pp. 317–328, Jan. 2016.
- [35] IBM. *Ibm Ilog Cplex Optimization Studio 12.5*. Accessed on Feb. 15, 2015. [Online]. Available: http://www-01.ibm.com/support/knowledgecenter/SSSA5P_12.5.1/maps/ic-homepage.html
- [36] X. Zhou and H. S. Mahmassani, "Dynamic origin-destination demand estimation using automatic vehicle identification data," *IEEE Trans. Intell. Transp. Syst.*, vol. 7, no. 1, pp. 105–114, Mar. 2006.
- [37] G. Li and X.-P. Zhang, "Modeling of plug-in hybrid electric vehicle charging demand in probabilistic power flow calculations," *IEEE Trans. Smart Grid*, vol. 3, no. 1, pp. 492–499, Mar. 2012.



Hongcai Zhang (S'14) received the B.S. degree in electrical engineering from Tsinghua University, Beijing, China, in 2010, where he is currently pursuing the Ph.D. degree in electrical engineering. He is currently an Exchange Student Researcher with the Energy, Controls, and Applications Laboratory, University of California, Berkeley.

His current research interests include electric vehicles grid integration, charging station planning, and demand response.

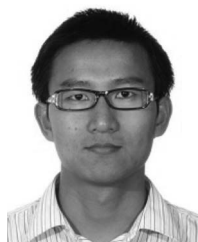


Scott J. Moura (S'09–M'13) received the B.S. degree from the University of California, Berkeley, CA, USA, in 2006, and the M.S. and Ph.D. degrees from the University of Michigan, Ann Arbor, MI, USA, in 2008 and 2011, respectively, all in mechanical engineering.

He is currently an Assistant Professor and the Director of the Energy, Controls, and Applications Laboratory (eCAL) in Civil & Environmental Engineering, University of California, Berkeley. From 2011 to 2013, he was a Post-Doctoral Fellow

with the Cymer Center for Control Systems and Dynamics, University of California, San Diego. In 2013, he was a Visiting Researcher with the Centre Automatique et Systèmes, MINES ParisTech, Paris, France. His current research interests include optimal and adaptive control, partial differential equation control, batteries, electric vehicles, and energy storage.

Dr. Moura was a recipient of the National Science Foundation Graduate Research Fellowship, the UC Presidential Post-Doctoral Fellowship, the O. Hugo Shuck Best Paper Award, the ACC Best Student Paper Award (as an Advisor), the ACC and ASME Dynamic Systems and Control Conference Best Student Paper Finalist (as a student), the Hellman Fellows Fund, the University of Michigan Distinguished ProQuest Dissertation Honorable Mention, the University of Michigan Rackham Merit Fellowship, and the College of Engineering Distinguished Leadership Award.



Zechun Hu (M'09) received the B.S. and Ph.D. degrees in electrical engineering from Xi'an Jiao Tong University, Xi'an, China, in 2000 and 2006, respectively.

He was with Shanghai Jiao Tong University, and the University of Bath as a Research Officer from 2009 to 2010. He joined the Department of Electrical Engineering, Tsinghua University, in 2010, where he is currently an Associate Professor. His major research interests include optimal planning and operation of power systems, electric vehicles, and energy storage systems.



Yonghua Song (F'08) received the B.E. degree from the Chengdu University of Science and Technology, Chengdu, China, in 1984, and the Ph.D. degree from China Electric Power Research Institute, Beijing, China, in 1989, all in electrical engineering.

From 1989 to 1991, he was a Post-Doctoral Fellow with Tsinghua University, Beijing. He then held various positions with Bristol University, Bristol, U.K., Bath University, Bath, U.K., and John Moores University, Liverpool, U.K., from 1991 to 1996. In 1997, he was a Professor of Power Systems with Brunel University, where he has been a Pro-Vice Chancellor for Graduate Studies since 2004. In 2007, he took up a Pro-Vice Chancellorship and Professorship of Electrical Engineering with the University of Liverpool, Liverpool. He was a Professor with the Department of Electrical Engineering, Tsinghua University, where he was an Assistant President and the Deputy Director of the Laboratory of Low-Carbon Energy in 2009. In 2012, he became the Executive Vice-President of Zhejiang University. His current research interests include smart grid, electricity economics, and operation and control of power systems.

Prof. Song was a recipient of the D.Sc. Award by Brunel University, in 2002, for his original achievements in power system research. He was elected as the Vice-President of the Chinese Society for Electrical Engineering (CSEE) and appointed as the Chairman of the International Affairs Committee of the CSEE in 2009. In 2004, he was elected as a fellow of the Royal Academy of Engineering, U.K.